GEOARCHAEOLOGICAL XRF LAB
GEOARCHAEOLOGICAL X-RAY FLUORESCENCE SPECTROMETRY LABORATORY
8100 WYOMING BLVD., SUITE M4-158 ALBUQUERQUE, NM 87113 USA

SOURCE PROVENANCE OF OBSIDIAN ARTIFACTS FROM ARCHAEOLOGICAL CONTEXTS IN DARK CANYON, CATRON COUNTY, NEW MEXICO

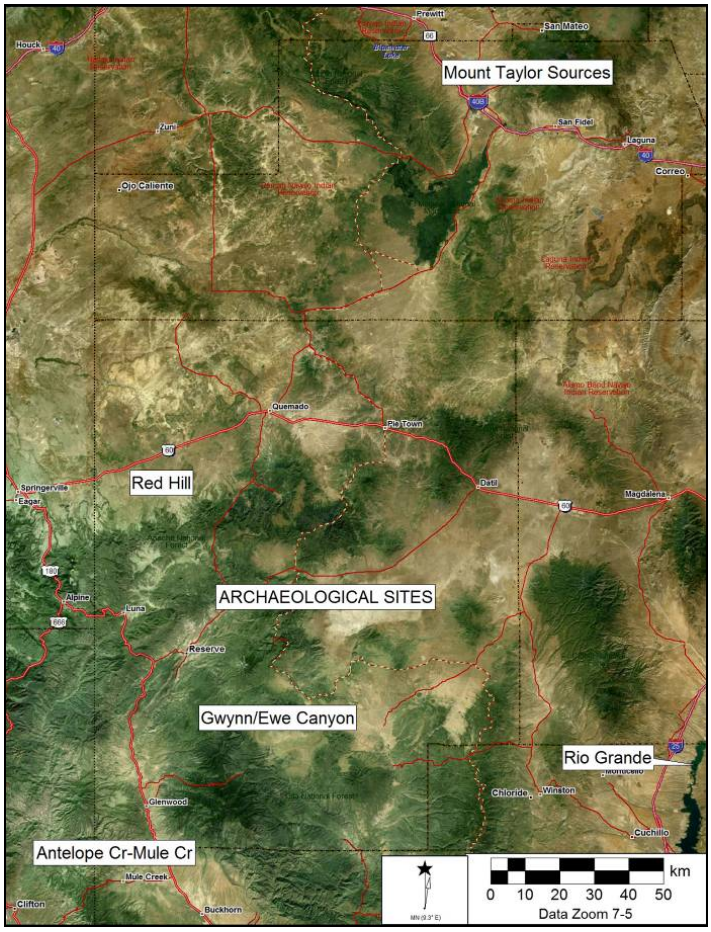

Digital elevation model of site locations and approximate obsidian source locations. Cerro Toledo Rhyolite source off sheet to northeast.

by

M. Steven Shackley Ph.D., Director
Geoarchaeological XRF Laboratory
Albuquerque, New Mexico

Report Prepared for

Matthew Taliaferro
Gila National Forest
Reserve, New Mexico

1 August 2015

INTRODUCTION

The analysis here of 19 obsidian artifacts from four sites in Dark Canyon indicates a diverse assemblage from sources both north and south of the sites. One of the nearest sources, Gwynn/Ewe Canyons in the Mogollon Highlands comprises nearly 50% of the assemblage overall, and Red Hill about the same distance north is present as only one sample (see discussion below).

LABORATORY SAMPLING, ANALYSIS AND INSTRUMENTATION

All archaeological samples are analyzed whole. The results presented here are quantitative in that they are derived from "filtered" intensity values ratioed to the appropriate x-ray continuum regions through a least squares fitting formula rather than plotting the proportions of the net intensities in a ternary system (McCarthy and Schamber 1981; Schamber 1977). Or more essentially, these data through the analysis of international rock standards, allow for inter-instrument comparison with a predictable degree of certainty (Hampel 1984; Shackley 2011).

All analyses for this study were conducted on a ThermoScientific *Quant'X* EDXRF spectrometer, located in the Geoarchaeological XRF Laboratory, Albuquerque, New Mexico. It is equipped with a thermoelectrically Peltier cooled solid-state Si(Li) X-ray detector, with a 50 kV, 50 W, ultra-high-flux end window bremsstrahlung, Rh target X-ray tube and a 76 μm (3 mil) beryllium (Be) window (air cooled), that runs on a power supply operating 4-50 kV/0.02-1.0 mA at 0.02 increments. The spectrometer is equipped with a 200 l min^{-1} Edwards vacuum pump, allowing for the analysis of lower-atomic-weight elements between sodium (Na) and titanium (Ti). Data acquisition is accomplished with a pulse processor and an analogue-to-digital converter. Elemental composition is identified with digital filter background removal, least squares empirical peak deconvolution, gross peak intensities and net peak intensities above background.

The analysis for mid Zb condition elements Ti-Nb, Pb, Th, the x-ray tube is operated at 30 kV, using a 0.05 mm (medium) Pd primary beam filter in an air path at 200 seconds livetime to generate x-ray intensity Ka-line data for elements titanium (Ti), manganese (Mn), iron (as $Fe_2O_3^T$), cobalt (Co), nickel (Ni), copper, (Cu), zinc, (Zn), gallium (Ga), rubidium (Rb), strontium (Sr), yttrium (Y), zirconium (Zr), niobium (Nb), lead (Pb), and thorium (Th). Not all these elements are reported since their values in many volcanic rocks are very low. Trace element intensities were converted to concentration estimates by employing a least-squares calibration line ratioed to the Compton scatter established for each element from the analysis of international rock standards certified by the National Institute of Standards and Technology (NIST), the US. Geological Survey (USGS), Canadian Centre for Mineral and Energy Technology, and the Centre de Recherches Pétrographiques et Géochimiques in France (Govindaraju 1994). Line fitting is linear (XML) for all elements but Fe where a derivative fitting is used to improve the fit for iron and thus for all the other elements. When barium (Ba) is analyzed in the High Zb condition, the Rh tube is operated at 50 kV and up to 1.0 mA, ratioed to the bremsstrahlung region (see Davis 2011; Shackley 2011). Further details concerning the petrological choice of these elements in Southwest obsidians is available in Shackley (1988, 1995, 2005; also Mahood and Stimac 1991; and Hughes and Smith 1993). Nineteen specific pressed powder standards are used for the best fit regression calibration for elements Ti-Nb, Pb, Th, and Ba, include G-2 (basalt), AGV-2 (andesite), GSP-2 (granodiorite), SY-2 (syenite), BHVO-2 (hawaiite), STM-1 (syenite), QLO-1 (quartz latite), RGM-1 (obsidian), W-2 (diabase), BIR-1 (basalt), SDC-1 (mica schist), TLM-1 (tonalite), SCO-1 (shale), NOD-A-1 and NOD-P-1 (manganese) all US Geological Survey standards, NIST-278 (obsidian), U.S. National Institute of Standards and Technology, BE-N (basalt) from the Centre de Recherches Pétrographiques et

Géochimiques in France, and JR-1 and JR-2 (obsidian) from the Geological Survey of Japan (Govindaraju 1994).

The data from the WinTrace software were translated directly into Excel for Windows software for manipulation and on into SPSS for Windows (ver. 21) for statistical analyses. In order to evaluate these quantitative determinations, machine data were compared to measurements of known standards during each run. RGM-1 a USGS obsidian standard is analyzed during each sample run for obsidian artifacts to check machine calibration (Table 1). Source assignments were made by reference to Shackley (1995, 2005 and updated at http://swxrflab.net/swobsrcs.htm; see Tables 1 and 2 and Figures 1 and 2.

DISCUSSION

Since the archaeological contexts for these artifacts are somewhat mixed, and the sample size is relatively small, it is hazardous to derive confident inferences, but there are some intriguing patterns that deserve comment. Refer to the cover image for the discussion below.

First, the artifact produced from Cerro Toledo Rhyolite is an interior flake (no cortex). It is tempting to infer that this is the greatest distance to source in the assemblage, but this source has been eroding into the Rio Grande since the eruptive event 1.4 mya (Church 2000, Shackley 2005, 2014). It is small enough to have certainly been procured from Quaternary Rio Grande alluvium to the east (see cover image).

The Gwynn/Ewe Canyon source is a Tertiary marekanite source at relatively high elevation generally too high for reliable agriculture, but rich in artiodactyls including deer, elk, and possibly bighorn sheep in prehistory (Shackley 2005; see http://swxrflab.net/gwyncyn.htm). There are a number of hunting camps in the source area. While it is not as commonly recovered in Archaic through Late Classic sites in the region as Antelope Creek at Mule Creek, also present here at about 1/3 of the assemblage, it is nevertheless present in good quantities regionally, and

likely represents embedded procurement alongside hunting at this high elevation source area (Mills et al. 2013).

The Mount Taylor sources (Grants Ridge and Horace/La Jara Mesas) are located in piñon/juniper woodlands with a high density of Archaic sites representing hunting and piñon gathering (Shackley 2005; http://swxrflab.net/grants.htm). This is a source commonly recovered in Archaic through contact period sites throughout New Mexico and western Arizona (Shackley 2005).

The Red Hill source, an excellent toolstone that exhibits nodule sizes up to at least 12 cm in diameter is somewhat of a conundrum in Southwestern archaeology (Shackley 2005; http://swxrflab.net/redhill.htm). It was not commonly used even in sites near the source, and the source is distributed over a large area (Duff et al. 2012). The sites in this study seem to conform to that pattern, since it is one of the nearest sources (see cover image).

REFERENCES CITED

Church, T.
2000 Distribution and Sources of Obsidian in the Rio Grande Gravels of New Mexico. *Geoarchaeology* 15:649-678.

Davis, K.D., T.L. Jackson, M.S. Shackley, T. Teague, and J.H. Hampel
2011 Factors Affecting the Energy-Dispersive X-Ray Fluorescence (EDXRF) Analysis of Archaeological Obsidian. In *X-Ray Fluorescence Spectrometry (XRF) in Geoarchaeology*, edited by M.S. Shackley, pp. 45-64. Springer, New York.

Duff, A.I., J.M. Moss, T.C. Windes, J. Kantner, and M.S. Shackley
2012 Patterning in Procurement of Obsidian in Chaco Canyon and in Chaco-era Communities in New Mexico as Revealed by X-Ray Fluorescence. *Journal of Archaeological Science*, 39:2995-3007.

Hampel, Joachim H.
1984 Technical Considerations in X-ray Fluorescence Analysis of Obsidian. In *Obsidian Studies in the Great Basin*, edited by R.E. Hughes, pp. 21-25. Contributions of the University of California Archaeological Research Facility 45. Berkeley.

Hildreth, W.
1981 Gradients in Silicic Magma Chambers: Implications for Lithospheric Magmatism. *Journal of Geophysical Research* 86:10153-10192.

Hughes, Richard E., and Robert L. Smith
1993 Archaeology, Geology, and Geochemistry in Obsidian Provenance Studies. *In Scale on Archaeological and Geoscientific Perspectives*, edited by J.K. Stein and A.R. Linse, pp. 79-91. Geological Society of America Special Paper 283.

Mahood, Gail A., and James A. Stimac
1990 Trace-Element Partitioning in Pantellerites and Trachytes. *Geochemica et Cosmochimica Acta* 54:2257- 2276.

McCarthy, J.J., and F.H. Schamber
1981 Least-Squares Fit with Digital Filter: A Status Report. In *Energy Dispersive X-ray Spectrometry*, edited by K.F.J. Heinrich, D.E. Newbury, R.L. Myklebust, and C.E. Fiori, pp. 273-296. National Bureau of Standards Special Publication 604, Washington, D.C.

Mills, B.J., J.J. Clark, M.A. Peeples, W.R. Haas, Jr., J.M. Roberts, Jr., J.B. Hill, D.L. Huntley, L. Borck, R.L. Breiger, A. Clauset, and M.S. Shackley
2013 Transformation of Social Networks in the Late Pre-Hispanic US Southwest. *PNAS* 110:5785-5790.

Schamber, F.H.
1977 A Modification of the Linear Least-Squares Fitting Method which Provides Continuum Suppression. In *X-ray Fluorescence Analysis of Environmental Samples*, edited by T.G. Dzubay, pp. 241-257. Ann Arbor Science Publishers.

Shackley, M. Steven
1988 Sources of Archaeological Obsidian in the Southwest: An Archaeological, Petrological, and Geochemical Study. *American Antiquity* 53(4):752-772.

1995 Sources of Archaeological Obsidian in the Greater American Southwest: An Update and Quantitative Analysis. *American Antiquity* 60(3):531-551.

2005 *Obsidian: Geology and Archaeology in the North American Southwest*. University of Arizona Press, Tucson.

2011 An Introduction to X-Ray Fluorescence (XRF) Analysis in Archaeology. In *X-Ray Fluorescence Spectrometry (XRF) in Geoarchaeology*, edited by M.S. Shackley, pp. 7-44. Springer, New York.

2014 Elemental and isotopic variability in Mogollon-Datil Volcanic Province obsidian, western New Mexico: issues in XRF analysis. Poster presented at the 40th International Symposium on Archaeometry, Los Angeles.

Table 1. Elemental concentrations and source assignments for the archaeological specimens by site, and the USGS RGM-1 obsidian standard. All measurements in parts per million (ppm).

Sample	Site	Ti	Mn	Fe	Zn	Rb	Sr	Y	Zr	Nb	Source
689-1	LA66799	704	468	12009	170	196	8	62	164	93	Cerro Toledo Rhy
689-2	LA66799	921	406	11145	106	220	22	27	146	26	Gwynn/Ewe Canyon
689-3	LA66799	713	391	11760	119	252	22	37	110	28	Antelope Cr-Mule Cr
690-1	LA66800	1072	414	11648	66	230	23	31	151	21	Gwynn/Ewe Canyon
690-2	LA66800	932	417	11231	74	225	24	30	156	28	Gwynn/Ewe Canyon
690-3	LA66800	385	687	10914	218	522	11	76	108	180	Grants Ridge-Mt Taylor
690-4	LA66800	579	352	11447	101	234	22	38	107	24	Antelope Cr-Mule Cr
690-5	LA66800	518	356	11372	70	238	18	38	107	23	Antelope Cr-Mule Cr
1344-1	LA156312	905	379	10998	57	222	22	32	151	21	Gwynn/Ewe Canyon
1344-2	LA156312	633	371	11561	47	233	21	42	108	24	Antelope Cr-Mule Cr
1344-3	LA156312	632	331	11282	44	221	19	44	105	27	Antelope Cr-Mule Cr
1344-4	LA156312	636	393	11739	57	236	21	39	108	26	Antelope Cr-Mule Cr
1344-5	LA156312	988	413	11384	55	226	23	32	147	24	Gwynn/Ewe Canyon
1345-1	LA156313	440	556	11639	257	495	10	79	129	221	Horace/La Jara Mesa-Mt Taylor
1345-2	LA156313	964	408	11431	61	223	21	30	142	24	Gwynn/Ewe Canyon
1345-3	LA156313	637	506	10732	40	164	15	40	66	45	Red Hill
1345-4	LA156313	1060	429	11435	53	230	19	31	149	23	Gwynn/Ewe Canyon
1345-5	LA156313	1010	449	11427	60	227	22	32	152	21	Gwynn/Ewe Canyon
1345-6	LA156313	921	425	11166	54	220	24	32	152	21	Gwynn/Ewe Canyon
RGM1-S4		1573	287	13745	34	149	106	23	215	8	standard

Table 2. Crosstabulation of site by source.

			Site				
			LA156312	LA156313	LA66799	LA66800	Total
Source	Antelope Cr-Mule Cr	Count	3	0	1	2	6
		% within Source	50.0%	0.0%	16.7%	33.3%	100.0%
		% within Site	60.0%	0.0%	33.3%	40.0%	31.6%
		% of Total	15.8%	0.0%	5.3%	10.5%	31.6%
	Gwynn/Ewe Canyon	Count	2	4	1	2	9
		% within Source	22.2%	44.4%	11.1%	22.2%	100.0%
		% within Site	40.0%	66.7%	33.3%	40.0%	47.4%
		% of Total	10.5%	21.1%	5.3%	10.5%	47.4%
	Grants Ridge-Mt Taylor	Count	0	0	0	1	1
		% within Source	0.0%	0.0%	0.0%	100.0%	100.0%
		% within Site	0.0%	0.0%	0.0%	20.0%	5.3%
		% of Total	0.0%	0.0%	0.0%	5.3%	5.3%
	Horace/La Jara Mesa-Mt Taylor	Count	0	1	0	0	1
		% within Source	0.0%	100.0%	0.0%	0.0%	100.0%
		% within Site	0.0%	16.7%	0.0%	0.0%	5.3%
		% of Total	0.0%	5.3%	0.0%	0.0%	5.3%
	Red Hill	Count	0	1	0	0	1
		% within Source	0.0%	100.0%	0.0%	0.0%	100.0%
		% within Site	0.0%	16.7%	0.0%	0.0%	5.3%
		% of Total	0.0%	5.3%	0.0%	0.0%	5.3%
	Cerro Toledo Rhy	Count	0	0	1	0	1
		% within Source	0.0%	0.0%	100.0%	0.0%	100.0%
		% within Site	0.0%	0.0%	33.3%	0.0%	5.3%
		% of Total	0.0%	0.0%	5.3%	0.0%	5.3%
Total		Count	5	6	3	5	19
		% within Source	26.3%	31.6%	15.8%	26.3%	100.0%
		% within Site	100.0%	100.0%	100.0%	100.0%	100.0%
		% of Total	26.3%	31.6%	15.8%	26.3%	100.0%

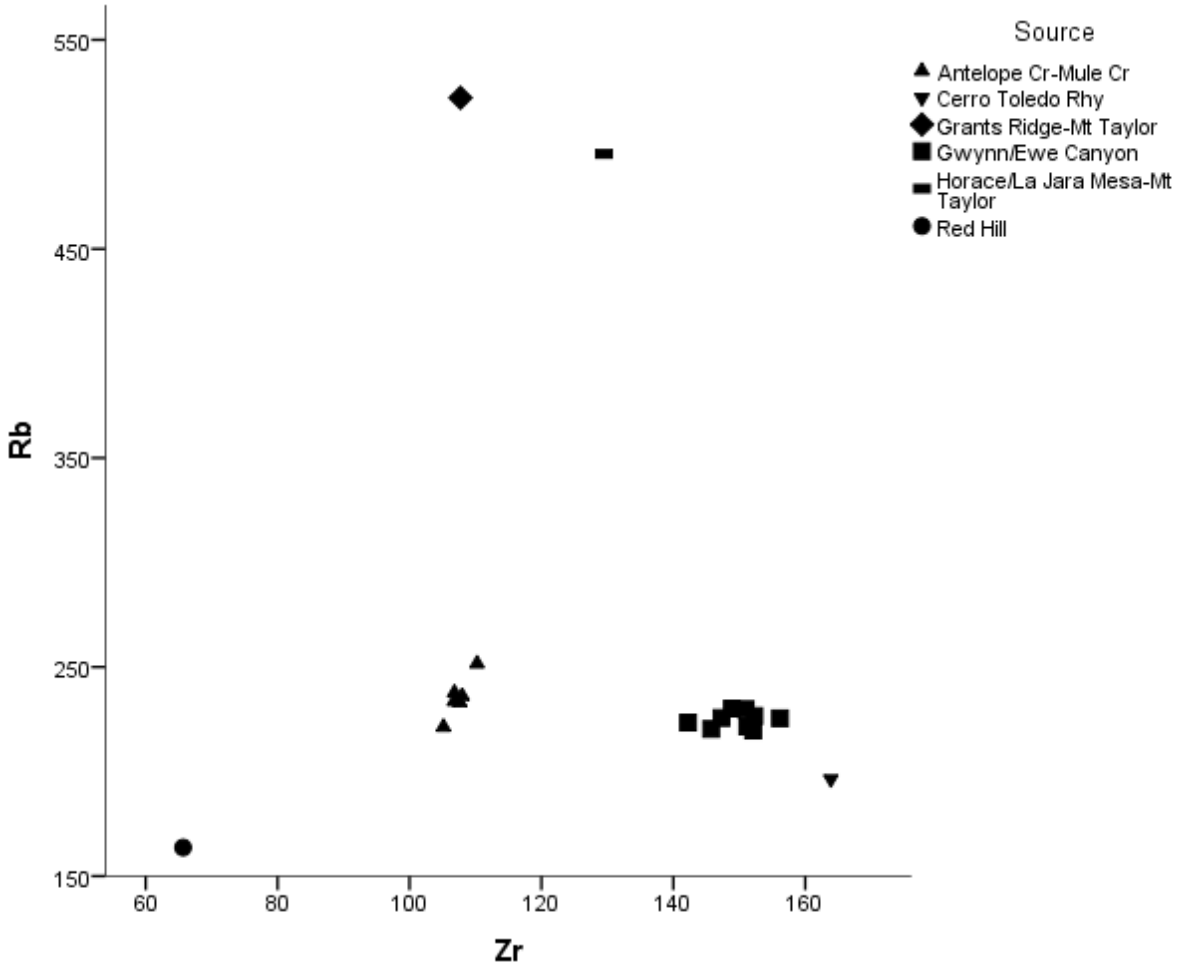

Figure 1. Zr versus Rb bivariate plot of the elemental concentrations for all the archaeological specimens from all sites. See plot below providing clarity for lower Rb concentration samples.

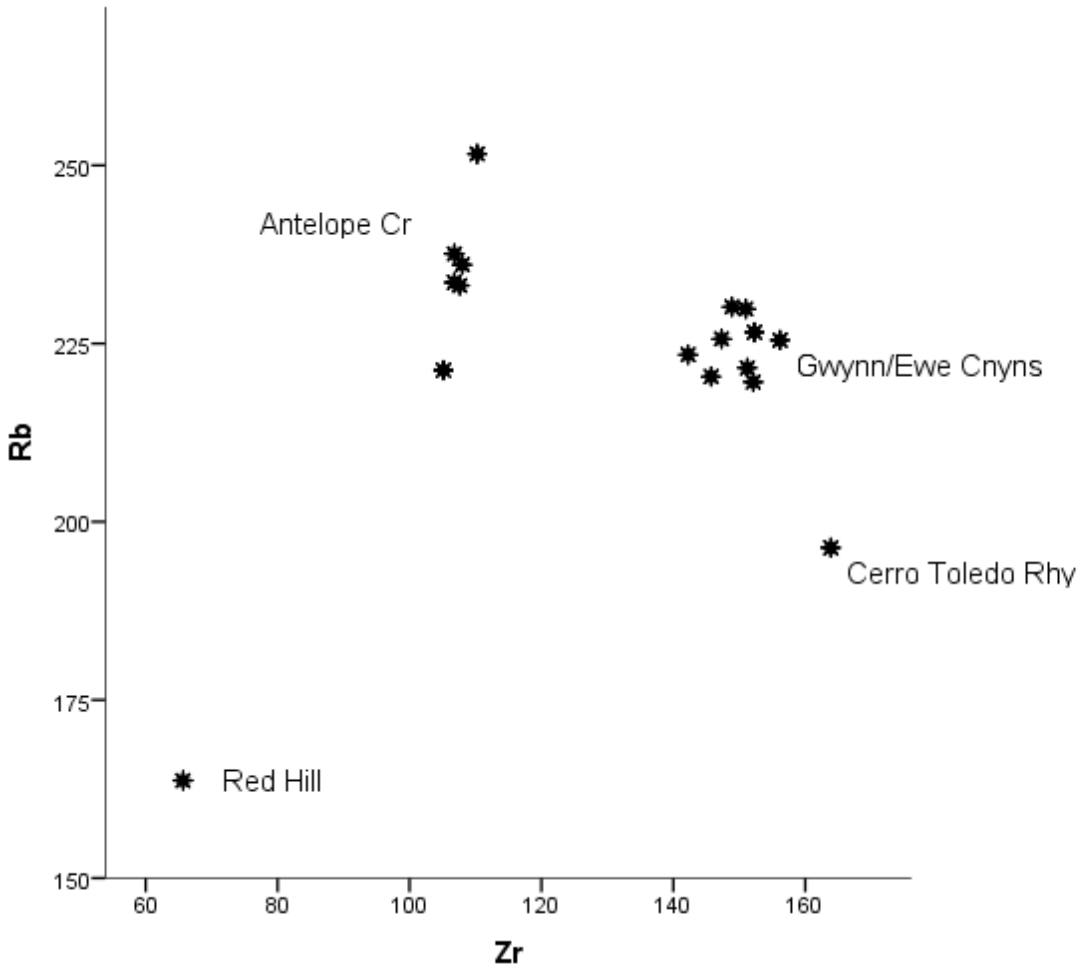

Figure 2. Zr versus Rb bivariate plot of the lower Rb concentration samples providing clarity.